Saharinen, Heloterä et al.

Supplemental Data

Supplemental materials and methods

Cell culture, reagents, immunoblotting, immunofluorescence. Madin-Darby canine kidney (MDCK), 293T (American Type Culture Collection) and Eahy.926 (Edgell et al. 1983) cells were grown in DMEM supplemented with 10% fetal bovine serum (FBS; PromoCell), glutamine and antibiotics. Human dermal microvascular endothelial cells (HDMEC), human dermal microvascular lymphatic (LECs) and blood vascular endothelial cells (BECs) (Makinen et al. 2001), human umbilical vein endothelial cells (HUVECs), human intestinal lymphatic endothelial cells (iLECs) (Norrmen et al. 2009) and human dermal microvascular endothelial cells immortalized with the SV40 Large T antigen (HMEC-1) (Ades et al. 1992) were grown in Endothelial Cell Basal Medium (PromoCell) with supplements provided by the manufacturer. Cells were kept at 37°C in a humidified atmosphere with 5% CO2. For hypoxic exposure, cells were incubated at 1% O_2 in a hypoxia chamber or the hypoxia response was chemically activated by exposure of cells to 250 μM cobalt chloride ($CoCl_2$). Cells were serum-starved for 2 to 4 hours or overnight, followed by stimulation with 100 ng/ml VEGF-A (R&D Systems), VEGF-E (Gerhardt et al. 2003) or VEGF-C (prepared by M.J.) or 200 ng/ml COMP-Ang1 (a kind gift from Dr. Gou Young Koh) (Cho et al. 2004). The following antibodies were used: anti-human VEGFR-2 (AF357), anti-mouse VEGFR-2 (AF644) and anti-Tie2 (R&D Systems), anti-human VEGFR-3 (9D9) (Jussila et al. 1998; Valtola et al. 1999), anti-mouse LYVE-1 (Petrova et al. 2004), anti-cAMP-responsive element binding protein (CREB) and anti-phospho-CREB (Ser133) (Cell Signaling), anti-mouse CD31

(PECAM-1) (BD Biosciences Pharmingen), anti-α-smooth muscle actin-Cy3 (Sigma), anti-V5 (Invitrogen), anti-β-Catenin (Upstate), anti-GFP (Invitrogen), anti-Prox1 (Karkkainen et al. 2004), and secondary antibodies conjugated to Alexa fluorochromes (Molecular Probes). Lipophilic carbocyanine dye (DiI, Invitrogen) staining for blood vasculature was done as previously described (Li et al. 2008).

Mouse lung endothelial cells were isolated as previously reported (Reynolds and Hodivala-Dilke 2006). Briefly, minced lungs were digested in collagenase type 1 (Gibco), passed through a 70 μm pore size cell strainer (BD Falcon) and plated on tissue culture plates coated with 0.1% gelatin containing 10 μg/ml fibronectin (Sigma). ~80% confluent plates were immunosorted using rat anti-mouse CD16/CD32 (Fcγ receptor) antibodies (AbD Serotech) to remove macrophages and endothelial cells were sorted twice using rat anti-mouse ICAM-2 antibodies (AbD Serotech). Cells were cultured at 37^{o}C in humidified atmosphere of 8% CO_2 in air, in a 50:50 mix of Hams F12 and DMEM media supplemented with 20% FBS, 6 mM glutamine, 100 μg/ml endothelial mitogen (Biogenesis), 1 μg/ml heparin and antibiotics.

RNA isolation and Northern blotting. Total RNA was isolated using the RNeasy kit (Qiagen), electrophoresed, blotted and hybridized with ^{32}P-labeled cDNA probes. Human 12-Lane Multiple Tissue Northern Blots (BD Biosciences Clontech no. 7780-1 and 7785-1) were hybridized with a CLP24 cDNA probe according to the manufacturer`s instructions.

Zebrafish husbandry, cloning of zebrafish *clp24* and morpholino injections.

Zebrafish lines *Fli1:eGFP*^{y1} (Lawson and Weinstein 2002) and wild-type AB were maintained under standard laboratory conditions (Kimmel et al. 1995). Embryos were kept in 0.3x Danieau (embryo water) at 28°C.

Clp24 coding sequence was amplified from total cDNA. Primers were designed based on available genomic information (GenBank:BC122129; ENSEMBL gene ENSDARG00000045273). Gene-specific antisense morpholino oligos were purchased from Gene Tools (LLC, Corvallis). *Clp24* morpholinos were directed against the 5' untranslated region (clp24-UTR; 5'-TACGCTAACGCTGAGAGACGCTTAG-3') and the translational start site (clp24-ATG; 5'-GCACGGCCATACGCCCCCCCCAAAA-3') of the *Clp24* gene. As a negative control we made use of a standard control morpholino (Gene tools, LLC) or injection solution (0.1% phenol red). Morpholinos were injected into single- to two-cell stage zebrafish embryos, using procedures as previously described (Lu et al. 2004) and embryos were further incubated in embryo water at 28°C.

***In situ* hybridization and scoring of thoracic duct and PL formation in zebrafish embryos.** For whole-mount *in situ* hybridization, dechorionated embryos were fixed overnight in 4% paraformaldehyde at 4°C. *In situ* hybridization using an antisense probe for *Clp24* was performed as described (Chittenden et al. 2006). Live screening and quantification of thoracic duct formation was performed on anaesthetized embryos (a few drops of 4 mg/ml Tricaine (Sigma) stock solution in 5 ml embryo water) of transgenic *Fli1:eGFP*^{y1} zebrafish with GFP expression in the blood and lymphatic vasculature (Kuchler et al. 2006; Lawson and Weinstein 2002; Yaniv et al.

2006). The percentage of thoracic duct formation was quantified at 6 dpf by scoring its percentile presence in 10 consecutive trunk to caudal somite segments from the junction of dorsal aorta (DA) and posterior cardinal vein (PCV) (i.e. somites 5-15). For screening of thoracic duct formation only embryos with normal overall morphology and normal trunk circulation were included. Because the penetrance of the lymphatic phenotype was variable, we also determined the fraction of embryos with severe, intermediate or subtle lymphatic defects per treatment condition. Chi-square analysis was used to determine whether the severity distribution differed between treatment groups. Screening of parachordal lymphangioblast (PL) cord (Hogan et al. 2009) formation in the 10-somite segment of the trunk was performed in a similar manner at 2 dpf.

In situ **hybridization, morpholino injections, morphometric and general analysis of the development in *Xenopus laevis*.** Fertilized *Xenopus laevis* one-cell stage eggs, purchased from Nasco Biology (Fort Atkinson, WI), were injected with 20-60 ng of morpholino (Gene Tools, Philomath, OR). Alternatively, embryos from a novel transgenic *Tg(Flk1:eGFP) Xenopus laevis* line, expressing GFP in the blood and lymphatic vasculature, were used. To design the ATG-targeted antisense morpholino for *clp24* (5'-CATGCCCATGCCTGTTCCTTTGGAC-3') the *Xenopus laevis* orthologue of *clp24* was first isolated from a cDNA library using the following primers: (forward) 5'-CAGAATGAGTGGGGATGTCCTCTAG-3' and (reverse) 5'-CCTTTGTGATTTCTGTGCCGCCATC -3'. Previously described morpholinos were used to knock down *vegfr3* (Ny et al. 2008); control embryos were injected with the standard control morpholino (SC, 5'- CCTCTTACCTCAGTTACAATTTATA-3') supplied by Gene Tools. The developing embryos were staged according to

Nieuwkoop and Faber (Nieuwkoop and Faber 1994) kept at 18°C until gastrulation was completed and from there on at 22°C.

To analyze the *prox1*-stained areas, images of the tail region of whole-mount tadpoles were acquired with the Zeiss AxioVision 4.6 software using an inverted Zeiss AxioVert 200M microscope equipped with a Zeiss AxioCam MrC5 digital camera and analyzed with the Zeiss KS300 morphometric analysis software with in-house–developed macros (Ny et al. 2005). Briefly, in the anterio-posterior axis, each region was defined from the location of the rectal diverticle to the tip of the tail; in the ventro-dorsal axis, area 1 was defined from the ventral border of the trunk to the dorsal margin of the endoderm, and area 2, from the dorsal margin of the endoderm to the dorsal border of the trunk. All analyses were performed by investigators blinded for the test condition, on tadpoles, matched for their stage and tail length. Stage-45 tadpoles were analyzed for the presence or absence of edema, heart beating, blood flow, and haemorrhage using a Zeiss SV11 stereomicroscope (Carl Zeiss). Statistical analysis was performed by using Fischer's Exact Test.

Analysis of blood vessels in *X. laevis*. Blood vessels were detected by in situ hybridization using probes for the blood vessel marker *msr* (gift from A. Ciau-Uitz of the Weatherall Institute of Molecular Medicine, Oxford, United Kingdom). Blood vessel formation was scored by counting the percentage of fully formed *msr*-positive intersomitic vessels (ISVs) reaching the dorsal roof and forming the dorsal longitudinal anastomosing vessel (DLAV) in the anterior trunk.

Mouse models. The offspring of *Clp24* gene targeted mice were genotyped using the following gene specific primers: 5'-AGTCCCTCCTGCTTAGAGCATACCC-3', 5'-ACCCTGACAAGCAACGCTACAGAGC-3' and 5'-AGAGTCTCCTGCACTGTCCGAAAGG-3'.

To confirm the absence of *Clp24* mRNA in *Clp24* gene targeted mice, total RNA was extracted from the intestine of wild type and *Clp24*$^{-/-}$ mice. cDNA synthesis was carried out using the Super Script VILO kit (Invitrogen) as described by the manufacturer. The resulting cDNA was amplified using gene-specific primers. The first primer pair (5` CAGGGGTAAGGGAGTCACAA 3` and 5` TTAGCCCAAGGATGAAGGTG 3`) annealed to exons 1 and 2, respectively, and produced a 206 bp fragment from the wild-type template. The second primer pair (5' ACAACTTTGGCATTGTGGAA 3' and 5' GATGCAGGGATGATGTTCTG 3') was specific for GAPDH cDNA and produced a 133 bp fragment from all samples confirming successful cDNA synthesis.

***In situ* hybridization (ISH) of mouse tissues**. The anti-sense and sense *Clp24* ISH probes were produced using the digoxigenin (DIG) labeling kit T7/SP6 according to the manufacturer's instructions (Roche). The probe concentration was quantified using a ready-to-use CDP-*Star*® Substrate (Applied Biosystems) according to the manufacturer's instructions, and the chemiluminescent signal produced was detected and quantified using a FluorChem HD2 Imaging system (Alpha Innotech).

16-30 μm cryosections were cut from mouse tissues embedded and frozen in Tissue Tek (Sakura Finetek). The cryosections were dried, fixed for 10 min at room temperature in 4% PFA in PBS, washed for 3 x 5 min in PBS, and acetylated for 10 min with constant stirring in 0.1 M triethanolamine (TEA) - 0.25 % acetic anhydride,

washed for 3 x 5 min in PBS. The cryosections were prehybridized at RT for 1-2 h in a hybridisation buffer (50% deionised formamide, 5x standard saline citrate (SSC), 5x Denhardt's solution, 500 μg/ml denaturated herring sperm DNA, 250 μg/ml yeast tRNA), followed by hybridization with 500 ng/ml of the *Clp24* probe in the hybridization buffer at +60-70 ^{o}C for 12-24 h in a humidifying chamber. The sections were then first rinsed with +52 ^{o}C 5x SSC, washed for 2 x 30 min at +65 ^{o}C with 0.2x SSC, rinsed once at room temperature with 0.2x SSC and washed for 5 min with Maleic acid buffer (0.1 M maleic acid, 0.15 M NaCl, pH 7.5). The sections were blocked for 1 h at room temperature using 1 % blocking reagent BMB (Roche) diluted into maleic acid buffer, and incubated for 1 h in 250 mU/ml alkaline phosphatase conjugated DIG antibody (Roche) diluted to 1 % BMB maleic acid buffer followed by washing 4 x 5 min in maleic acid buffer and 5 min in NTMT buffer (0.1 M Tris pH 9.5, 0.1 M $MgCl_2$, 0.1 M NaCl, 0.1 % Tween20 in aqua). The alkaline phosphatase substrate BM purple (Roche) with 0.25 mg/ml levamisole was added to the sections and the reaction was let to proceed overnight at room temperature, then stopped by washing 2 x 5 min with PBS, fixed with 4% PFA for 20 min and washed 2 x with PBS for 5 min. Finally, the sections were mounted using Aquamount (Lerner Laboratories). Whole mount ISH was performed as described (Petrova et al. 2004).

Supplemental References

Ades EW, Candal FJ, Swerlick RA, George VG, Summers S, Bosse DC, Lawley TJ. 1992. HMEC-1: establishment of an immortalized human microvascular endothelial cell line. J Invest Dermatol 99: 683-690.

Chittenden TW, Claes F, Lanahan AA, Autiero M, Palac RT, Tkachenko EV, Elfenbein A, Ruiz de Almodovar C, Dedkov E, Tomanek R et al. 2006. Selective regulation of arterial branching morphogenesis by synectin. Dev Cell 10: 783-795.

Cho CH, Kammerer RA, Lee HJ, Yasunaga K, Kim KT, Choi HH, Kim W, Kim SH, Park SK, Lee GM et al. 2004. Designed angiopoietin-1 variant, COMP-Ang1, protects against radiation-induced endothelial cell apoptosis. Proc Natl Acad Sci U S A 101: 5553-5558.

Edgell C-J, McDonald CC, Graham JB. 1983. Permanent cell line expressing human factor VII-related antigen established by hybridization. Proc Natl Acad Sci USA 50: 3734-3737.

Gerhardt H, Golding M, Fruttiger M, Ruhrberg C, Lundkvist A, Abramsson A, Jeltsch M, Mitchell C, Alitalo K, Shima D et al. 2003. VEGF guides angiogenic sprouting utilizing endothelial tip cell filopodia. J Cell Biol 161: 1163-1177.

Hogan BM, Bos FL, Bussmann J, Witte M, Chi NC, Duckers HJ, Schulte-Merker S. 2009. Ccbe1 is required for embryonic lymphangiogenesis and venous sprouting. Nat Genet 41: 396-398.

Jussila L, Valtola R, Partanen TA, Salven P, Heikkila P, Matikainen MT, Renkonen R, Kaipainen A, Detmar M, Tschachler E et al. 1998. Lymphatic endothelium and Kaposi's sarcoma spindle cells detected by antibodies against the vascular endothelial growth factor receptor-3. Cancer Res 58: 1599-1604.

Karkkainen MJ, Haiko P, Sainio K, Partanen J, Taipale J, Petrova TV, Jeltsch M, Jackson DG, Talikka M, Rauvala H et al. 2004. Vascular endothelial growth factor C is required for sprouting of the first lymphatic vessels from embryonic veins. Nat Immunol 5: 74-80.

Kimmel CB, Ballard WW, Kimmel SR, Ullmann B, Schilling TF. 1995. Stages of embryonic development of the zebrafish. Dev Dyn 203: 253-310.

Kuchler AM, Gjini E, Peterson-Maduro J, Cancilla B, Wolburg H, Schulte-Merker S. 2006. Development of the zebrafish lymphatic system requires VEGFC signaling. Curr Biol 16: 1244-1248.

Lawson ND, Weinstein BM. 2002. In vivo imaging of embryonic vascular development using transgenic zebrafish. Dev Biol 248: 307-318.

Li Y, Song Y, Zhao L, Gaidosh G, Laties AM, Wen R. 2008. Direct labeling and visualization of blood vessels with lipophilic carbocyanine dye DiI. Nat Protoc 3: 1703-1708.

Lu X, Le Noble F, Yuan L, Jiang Q, De Lafarge B, Sugiyama D, Breant C, Claes F, De Smet F, Thomas JL et al. 2004. The netrin receptor UNC5B mediates guidance events controlling morphogenesis of the vascular system. Nature 432: 179-186.

Makinen T, Veikkola T, Mustjoki S, Karpanen T, Catimel B, Nice EC, Wise L, Mercer A, Kowalski H, Kerjaschki D et al. 2001. Isolated lymphatic endothelial cells transduce growth, survival and migratory signals via the VEGF-C/D receptor VEGFR-3. Embo J 20: 4762-4773.

Nieuwkoop PJ, Faber J. 1994. Normal Table of Xenopus Laevis (Daudin): A Systematical and Chronological Survey of the Development from the Fertilized Egg till the End of Metamorphosis. . NY: Garand Publishing.

Norrmen C, Ivanov KI, Cheng J, Zangger N, Delorenzi M, Jaquet M, Miura N, Puolakkainen P, Horsley V, Hu J et al. 2009. FOXC2 controls formation and maturation of lymphatic collecting vessels through cooperation with NFATc1. J Cell Biol 185: 439-457.

Ny A, Koch M, Schneider M, Neven E, Tong RT, Maity S, Fischer C, Plaisance S, Lambrechts D, Heligon C et al. 2005. A genetic Xenopus laevis tadpole model to study lymphangiogenesis. Nat Med 11: 998-1004.

Ny A, Koch M, Vandevelde W, Schneider M, Fischer C, Diez-Juan A, Neven E, Geudens I, Maity S, Moons L et al. 2008. Role of VEGF-D and VEGFR-3 in developmental lymphangiogenesis, a chemicogenetic study in Xenopus tadpoles. Blood 112: 1740-1749.

Petrova TV, Karpanen T, Norrmen C, Mellor R, Tamakoshi T, Finegold D, Ferrell R, Kerjaschki D, Mortimer P, Yla-Herttuala S et al. 2004. Defective valves and abnormal mural cell recruitment underlie lymphatic vascular failure in lymphedema distichiasis. Nat Med 10: 974-981.

Reynolds LE, Hodivala-Dilke KM. 2006. Primary mouse endothelial cell culture for assays of angiogenesis. Methods Mol Med 120: 503-509.

Robu ME, Larson JD, Nasevicius A, Beiraghi S, Brenner C, Farber SA, Ekker SC. 2007. p53 activation by knockdown technologies. PloS Genet 3: 0787-0801.

Valtola R, Salven P, Heikkila P, Taipale J, Joensuu H, Rehn M, Pihlajaniemi T, Weich H, deWaal R, Alitalo K. 1999. VEGFR-3 and its ligand VEGF-C are associated with angiogenesis in breast cancer. Am J Pathol 154: 1381-1390.

Yaniv K, Isogai S, Castranova D, Dye L, Hitomi J, Weinstein BM. 2006. Live imaging of lymphatic development in the zebrafish. Nat Med 12: 711-716.

Supplemental Figure Legends

Supplemental Figure 1. Expression of *CLP24* in cultured endothelial cells and in human tissues. A) Expression of *CLP24* mRNA in cultured cells was analyzed by Northern blotting. B) Expression of *CLP24* mRNA in human tissues was analyzed in multiple tissue Northern blots (Clontech). C) Expression of *CLP24* mRNA in HMEC-1 cells under hypoxic conditions was analyzed by Northern blotting. D) Multiple alignment of the *H. sapiens* (NP_078876), *M. musculus* (NP_001001183), *G. gallus* (XP_415054), *X. tropicalis* (NP_001107367), *D. rerio* (NP_001157369) and *X. laevis* peptide sequences was calculated using CLUSTAL 2.0.12 multiple sequence alignment (EMBL-EBI website). The *X. laevis* sequence was translated from a cDNA amplified from a *X. laevis* cDNA pool (see Materials and Methods for details). E) Amino acid sequence similarities and identities of *X. laevis* clp24 and of indicated species were determined using EMBOSS pairwise alignment/Blosum62 Matrix on the EMBL-EBI website (http://www.ebi.ac.uk/embl/).

Supplemental Figure 2. Expression of *Clp24* in E15.5 mouse embryos and in microvascular endothelial cells. A-D) *Clp24* (A, C) and *Vegfr2* (B, D) *in situ* hybridization of E15.5 mouse embryos. Mouse brain (A, B) and forelimb (C, D). E, F) HDMECs were transfected with CLP24-EGFP (E) and CLP24-V5 (F) retroviruses and stained with anti-β-Catenin (red) and anti-V5 antibody (green in F). Nuclei are stained with DAPI.

Supplemental Figure 3. Expression of *Clp24* in E16.5 mouse embryos. A, B) *Clp24* (A) and *Vegfr2* (B) *in situ* hybridization of E16.5 mouse embryos. *Clp24* is expressed in blood vessels of e.g. the brain and the developing limb (Li). *Clp24* and *Vegfr2* are also highly expressed in the lung (L), but *Clp24* mRNA is absent from the neural retina (arrowhead) and brown fat (F), where *Vegfr2* is expressed. Magnification from the marked area is shown in Fig.1.

Supplemental Figure 4. *D. rerio* and *X. laevis clp24* sequences and blood vascular effects in *clp24* morpholino treated X. *laevis* embryos. A) *D. rerio clp24* mRNA sequence. Black, bold text indicates a morpholino (MO) targeted against the 5' untranslated region (*clp24*-UTR), blue underlined text indicates a MO (*clp24*-ATG) targeted against the translational start site (bold underlined) of *clp24* mRNA. *X. laevis* partial mRNA sequence. Underlined is a MO targeted against the 5' untranslated region, and in bold a MO targeted against the translational start site (bold underlined). B) Results from the experiments using the *D. rerio clp24*-ATG MO confirm the results obtained using the *clp24*-UTR MO, presented in Fig. 2. Toxic off-target effects of the second Clp24 MO assumably related to induction of a p53-dependent cell death pathway were attenuated by co-injection with a p53 morpholino as described (Robu et

al. 2007). C-F) Control (C, D) and *clp24* morpholino oligonucleotides (40 ng) (E, F) were injected into *X. laevis* embryos and the embryos were analyzed at st 33/34 by *in situ* hybridization with a *msr* probe staining the vasculature. At stage 32 *msr* was expressed in the heart and developing primary blood vessels. The *clp24* morphants show less staining in the dorsal aorta (DA) and in the posterior cardinal vein (PCV), and have less intersomitic vessel (ISV) sprouts as compared to the control (3.67 ± 0.39 (n=21) *vs* 4.1 ± 0.33 (n=20), respectively), although this decrease did not reach statistical significance.

Supplemental Figure 5. Conditional targeting of the *Clp24* locus. A) Schematic presentation of the *Clp24* gene. Exon 1 (red rectangles), LoxP (black triangles), FRT (orange circles), neomycin (Neo) positive selection cassette (green box), Diphteria Toxin A (DTA) negative selection marker (Grey box), AvrII restriction enzyme digestion sites and the binding site for the 5' Southern probe are indicated. B) Correct targeting of the *Clp24* locus was confirmed by 5' Southern blotting. Heterozygous founders are positive for both targeted allele (4.7kb) and wild type allele (9.5kb). C) Absence of *Clp24* mRNA in *Clp24* gene targeted mice was confirmed by RT-PCR. PCR using primers specific for *Clp24* gene exons 1 and 2 produced a 206 bp PCR product from cDNA produced from $Clp24^{+/+}$, but not from $Clp24^{-/-}$ mice (upper panel). A 133 bp PCR product was amplified with primers specific for the *Gapdh* gene exons 3 and 4. *Gapdh* transcripts were detected from both of the $Clp24^{+/+}$ *and* $Clp24^{-/-}$ mice.

Supplemental Figure 6. Increased numbers of smooth muscle cell (SMC) are associated with lymphatic vessels in $Clp24^{-/-}$ mice. A-D) Whole-mount staining of

the ear vasculature of *Clp24*$^{-/-}$ (A, C) and *Clp24*$^{+/+}$ (B, D) mice for LYVE-1 (white pseudocolor), VEGFR-2 (green) and SMA (red). A, B) LYVE-1 expression is downregulated in lymphatic vessels covered with SMA positive SMCs (arrows in A). C, D) The amount of SMC clusters associated with initial lymphatic vessels in the ear periphery (boxed area)(arrows in C) was calculated from similar sized 2.25 m^2 fields (C, D, results shown in Fig. 3F). A broken line marks the border of the ear. Collecting lymphatic vessels located deeper in the tissue were covered with continuous SMC layer (arrowheads). Scale bar 100 μm.

Supplemental Figure 7. Enlarged lymphatic vessels in the *Clp24* gene targeted mice with endothelial specific deletion of *Clp24*. Conditional *Clp24* gene targeted mice were crossed with Tie1-Cre mouse line to create endothelial specific deletion of *Clp24*. A, B) Whole-mount staining of lymphatic vessels for LYVE-1 in the ears of *Clp24 EC* $^{-/-}$ (A) and *Clp24 EC* $^{+/+}$ (B) mice.

Supplemental Figure 8. Genetic interaction between *Clp24* and *Vegfr2* and *Vegfr3* pathways in lymphatic vessel patterning. A-F) Whole-mount staining of lymphatic vessels for LYVE-1 in the ears of wild type (A), *Clp24*$^{-/-}$ (B), *Clp24*$^{+/-}$ *Vegfr3*$^{+/lz}$ (C), *Clp24*$^{-/-}$ *Vegfr3*$^{+/lz}$ (D) *Clp24*$^{+/-}$*Vegfr2*$^{+/lz}$ (E) and *Clp24*$^{-/-}$ *Vegfr2*$^{+/lz}$ (F) mice. The % increase in LYVE-1 positive area, versus wild type mice, indicated in each picture, was statistically significant in each case ($p<0.05$). Scale bar 100 μm. G-I) LacZ-staining of the heart (G), lung (H) and intestine (I) of *Clp24*$^{-/-}$*Vegfr3*$^{+/lz}$ and *Clp24*$^{+/-}$*Vegfr3*$^{+/lz}$ mice. Scale bars 100 μm (B, E) and 1 mm (G, H).

Supplemental Figure 9. Normal blood vasculature in *Clp24*$^{-/-}$ mice. A, B) DiI staining of intestinal vasculature of *Clp24*$^{-/-}$ and *Clp24*$^{-/+}$ mice. C-H) LacZ-staining of diaphragm (C, D), intestine (E, F) and thymus (G, H) from *Clp24*$^{-/-}$*Vegfr2*$^{+/lz}$ and *Clp24*$^{+/+}$*Vegfr2*$^{+/lz}$ mice. Note enlarged VEGFR-2 expressing lymphatic vessels in the diaphragm of *Clp24*$^{-/-}$*Vegfr2*$^{+/lz}$ mice (arrowheads in D).

Supplemental Figure 10. Control (SC, 70ng), *vegfr3* (50ng), *clp24* (20ng) and combination of *vegfr3*/*clp24* (Combo, 50ng + 20ng) MO oligonucleotide treated *X. laevis* tadpoles were analyzed at stage 46. Each MO was used at suboptimal levels, which did not induce or induced only minor defects when compared to controls. A) Edema formation in MO treated tadpoles. A suboptimal dose of *clp24* MO (20ng) did not increase edema formation (edema was seen in 11.3% of *clp24* morphants vs in 12.5% of control tadpoles). *Vegfr3* MO alone at a low dose (50ng) caused edema formation in 39% of the injected embryos. Combined injection of *vegfr3*-50ng + *clp24*-20ng dramatically increased edema formation to 89%. Taken together, these results show an additive effect of combined *clp24* and *vegfr3* knockdown on the formation of edema. B) *Tg(Flk1:eGFP)* reporter tadpoles were analysed for defects in development of the caudal lymphatic vessels. The graph shows the fraction of morphant tadpoles with normal lymphatic vessels, tadpoles with defects in the DLCV only, and tadpoles with defects in both DCLV and VCLV. Tadpoles with defects in the VCLV without having defects in the DCLV were never observed. Note additive effect of combined *clp24* and *vegfr3* knockdown on the formation of edema and severe lymphatic defects in all double MO injected embryos. Ventral caudal lymph vessel (VCLV), dorsal caudal lymphatic vessel (DCLV).

Supplemental Figure 11. Endothelial cells isolated from *Clp24*$^{-/-}$ mice express endothelial cell markers. A-F) Staining for VE-Cadherin (A, B), VEGFR-2 (C, D), VEGFR-3 and PECAM-1 (E, F) in *Clp24*$^{-/-}$ (A, C, E) and WT (B, D, F) mouse endothelial cells.

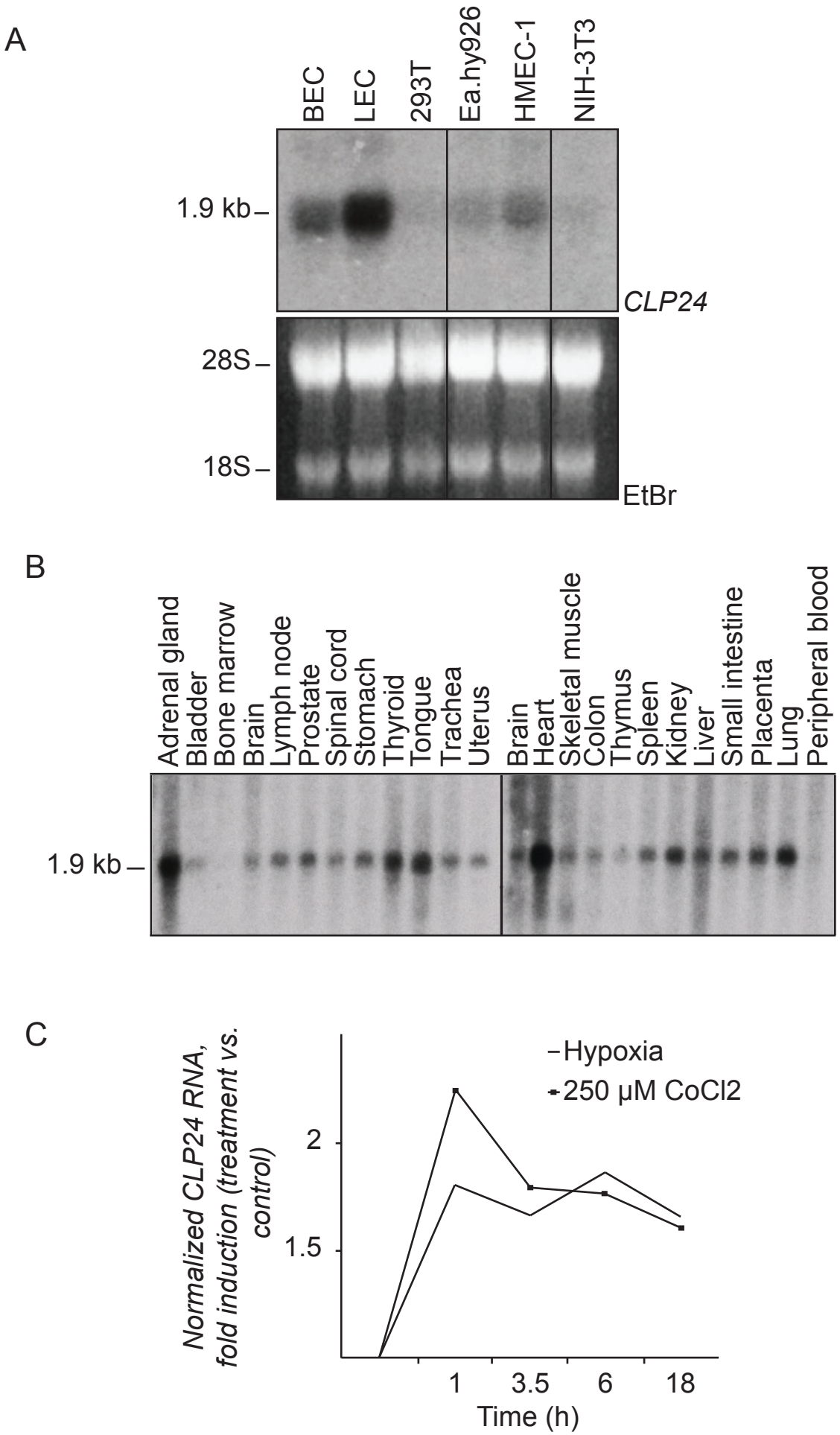
A
BEC
LEC
293T
Ea.hy926
HMEC-1
NIH-3T3
1.9 kb
CLP24
28S
18S
EtBr
B
Adrenal gland
Bladder
Bone marrow
Brain
Lymph node
Prostate
Spinal cord
Stomach
Thyroid
Tongue
Trachea
Uterus
Brain
Heart
Skeletal muscle
Colon
Thymus
Spleen
Kidney
Liver
Small intestine
Placenta
Lung
Peripheral blood
1.9 kb
C
Normalized CLP24 RNA, fold induction (treatment vs. control)
Hypoxia
250 µM CoCl2
2
1.5
1
3.5
6
18
Time (h)

D

Multiple alignment of Clp24 protein

```
H_sapiens       MTVQRLVAAAVLVALVSLILNNVAAFTSNWVCQTLEDGRRRSVGLWRSCWLVDRTRGGPS 60
M_musculus      MTLQKLVATAVLVALVSLILNNAAAFTPNWVYQTLEDGRKRSVGLWKSCWLVDRGKGVTS 60
G_gallus        MTVQKLVATAVLVALVSLILNNAAAFTPNWVYQTLEDGRKRSVGLWKMCWLAERSRAGAS 60
X_tropicalis    MGMQKLVAVAVVVALVSLVLNNVAAFTPNWVYQTLEEGRKRSVGLWKMCFTSKGVLGGN- 59
X_laevis        MGMQKLVAVAVVVALVSLVLNNVAAFTPNWVYQTLEEGRKRSVGLWKMCFTTKGVLAGN- 59
D_rerio         MAVRRLVELAAAVALLSLVLNSVATFSSGWVLQVLDDGRRRSVGLWRACVQED------- 53
                * :::**  *. ***:**:**..*:*:..** *.*::**:******: *   .

H_sapiens       PGARAGQVDAHDCEALGWGSEAAGFQESRGTVKLQFDMMRACNLVATAALTAGQLTFLLG 120
M_musculus      PGTRTGQVDTHDCEVLGWGSESAGFQESRGTVKLQFDMMRACNLVATAALVVGQITFILG 120
G_gallus        TSSRHGQGEERECEALGWGSESAGFQESRSTVKLQFDMMRACNLIATVALTAGQLIFVLG 120
X_tropicalis    --NRLGQGDERECHSLGWGSEPSGLQESRNTVKLQFDMMRACNLIATVALTAGQLIFLMG 117
X_laevis        --NRQGQGEERECHLLGWGSEPSGLQESRSTVKLQFDMMRACNLIATVALTAGQLIFLMG 117
D_rerio         ----THTHELTACQRLSWGSELAGYQESRSTVKLQFDMMRACNLMATVALTVGQLIFLFG 109
                          :   *. *.**** :* ****.***************:**.**..**: *::*

H_sapiens       LVGLPLLSPDAPCWEEAMAAAFQLASFVLVIGLVTFYRIGPYTNLSWSCYLNIGACLLAT 180
M_musculus      LTGLPLMSPESQCWEEAMAAAFQLASFVLVIGLVTFYRIGPYTNLSWSCYLNIGACLLAT 180
G_gallus        LVEIPIISQDTQWWEEAIAAVFQLASFVLVIGLVTFYRIGPYTNLSWSCYLNIGACLLAT 180
X_tropicalis    LIELPIVSQDSEWWEEAIAAVFQLASFVLVIGLVTFYRIGPYTHLSWSCYLDIVACLLAT 177
X_laevis        LIELPIVSQDSEWWEEAIAAVFQLASFVLVIGLVTFYRIGPYTHLSWSCYLDIVACLLAT 177
D_rerio         LLEISHITQDSQWWEEAIAALFQLASFVLVIGLVTFYRIGPYTHLSYSCYINIAACLFAT 169
                *  :. :: ::  ****:** **********************:**:***::* ***:**

H_sapiens       LAAAMLIWNILHKREDCMAPRVIVISRSLTARFRRGLDNDYVESPC 226
M_musculus      LAAAMLIWNILHRREDCMAPRVIVISRSLTARFRRGLDNDYVESPC 226
G_gallus        LAAAILIWNILHRREDCMAPRVIVISRTLTARFRRGLENDYVESPC 226
X_tropicalis    LAAAILIWNILHRREDCMAPRVIVISRTLTARFRRGLDNDYVESPC 223
X_laevis        LAAAILIWNILHRREDCMAPRVIVI---------------------- 202
D_rerio         LAAAMLIWNILHRRDDCLSPSVIVISRSLTTPFRPRLDNDYVESPC 215
                ****:*******:*:**::* ****
```

E

Amino acid sequence similarities and identities

		seq similarity (%)	*seq identity (%)*
X laevis Clp24 protein *versus*	H sapiens	77	66.4
	M musculus	77	67.3
	G gallus	83.2	75.2
	X tropicalis	89.2	87.9
	D rerio	71.9	60.3

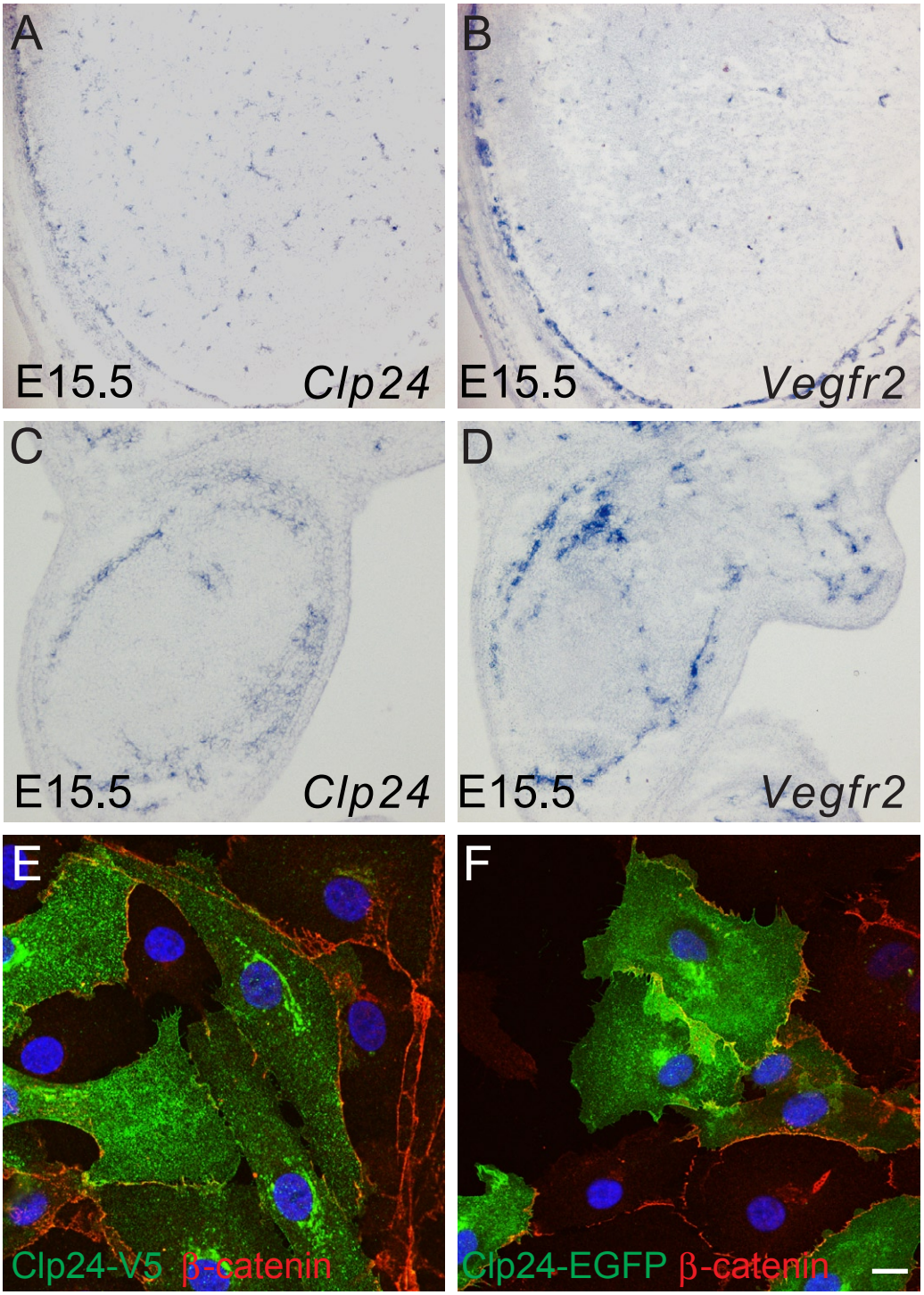
A
E15.5
Clp24
B
E15.5
Vegfr2
C
E15.5
Clp24
D
E15.5
Vegfr2
E
Clp24-V5 β-catenin
F
Clp24-EGFP β-catenin

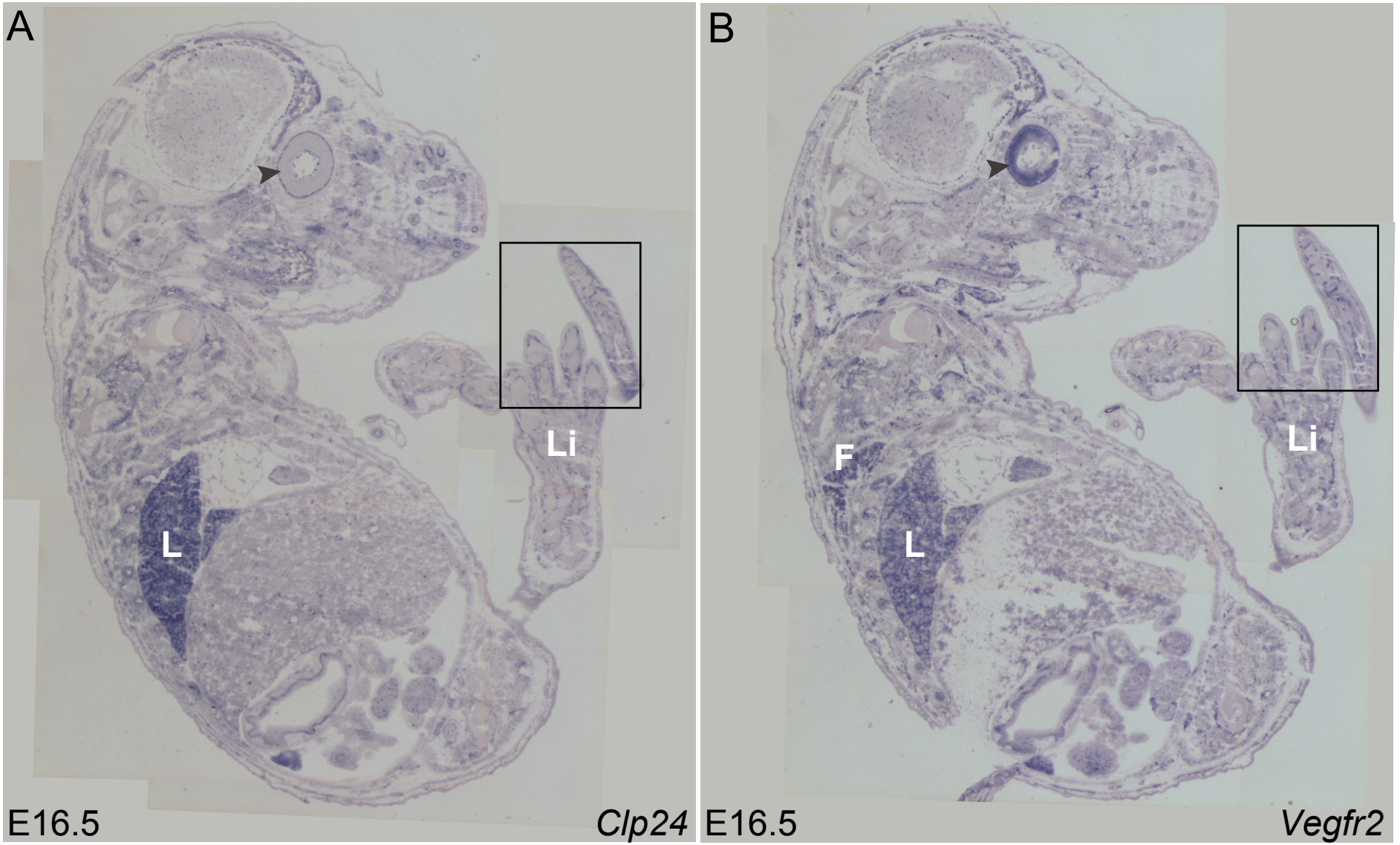
A
Li
L
E16.5
Clp24
B
F
L
Li
E16.5
Vegfr2

A

Danio rerio *clp24* mRNA sequence (NM_001163897)

```
   1  CATCCTGTAG ACGGAGCGAC GTATTTGTCA CACACAGAAA GCGAGACAGA GAGAGAGAGA
  61  GAGAGAGAGA GAGAGAGAGA GAGATAGGGA GAGTATTCCC AAGTCCACCC CACCATCTCA
 121  TCCCACTTCT TCTGAGCTTT TCAGGGATGA AACACGCGCG TGTTAACATG GGAAACACAG
 181  TGTGAGTAAT CTGAGCTCGC CGAGTGTGGG AAAGCAGCAC AGAGACGGCA TCACGCAGAC
 241  ATTCCTCAAC TTTCCCAGCA GGGAGACCTC AGAAAAAAAA ACAACCCAGA GCACATCTGC
 301  AGGAGCGAGG GGGAGGAAAC AAGACCTCAG AAAGAAATCC CAGAGATTTT GAGCAAGCGT
 361  GTGATGGCCT TGGAGGTCCA GCGTCCAGCA TTAAGAGCGA GCCCAGACTC TGAAGAAGAG
 421  GGATAGAGAC TACCTAACGA CACAAGAATG AGTGGCGATG TCCTCTAGCT AAGCGTCTCT
 481  CAGCGTTAGC GTAGGGTTTT TGGGGGGGGC GTATGGCCGT GCGCAGACTG GTGGAGTTGG
 541  CGGCGGCGGT TGCCCTGCTA TCTCTGGTGC TCAATAGCGT GGCGACGTTC AGCTCCGGCT
 601  GGGTGCTGCA GGTGCTGGAC GACGGACGGC GTCGCAGCGT TGGGCTCTGG AGAGCATGTG
 661  TGCAGGAGGA TACACACACT CATGAACTCA CAGCCTGCCA GAGACTGAGC TGGGGATCAG
 721  AGCTGGCGGG GTACCAGGAG TCTCGCAGCA CAGTCAAACT TCAGTTTGAC ATGATGCGGG
 781  CATGTAACCT GATGGCTACG GTGGCTCTGA CCGTGGGTCA GCTAATCTTC CTGTTTGGGT
 841  TACTGGAGAT AAGCCACATT ACCCAGGATT CTCAGTGGTG GGAGGAGGCC ATCGCTGCTC
 901  TGTTCCAGTT AGCCAGTTTT GTGTTGGTGA TCGGTCTGGT GACGTTCTAC AGGATCGGCC
 961  CCTATACTCA CCTCTCCTAC TCCTGCTACA TAAACATCGC CGCATGCTTA TTTGCCACGC
1021  TAGCAGCCGC CATGCTAATC TGGAATATTC TGCACCGCCG CGATGACTGT CTGTCGCCGT
1081  CTGTCATTGT CATCAGTCGA TCTTTAACTA CACCATTCAG GCCACGGCTG GACAATGACT
1141  ATGTTGAGTC ACCGTGCTGA
```

Xenopus laevis *clp24* mRNA sequence (partial)

```
CAGAATGAGTGGGGATGTCCTCTAGCCTCTCCTGACCCCGTGCAGTGCGGCAGGGGAGTCCCCAT
TTGAGGGGCCAAAAGTCCAAAGGAACAGGCATGGGCATGCAAAAGCTGGTGGCAGTGGCTGTGGT
CGTGGCTTTGGTATCACTGGTGCTCAACAATGTGGCYGCCTTCACACCTAACTGGGTGTACCAAA
CATTGGAAGAGGGGCGCAAGCGCAGCGTGGGGCTGTGGAAGATGTGCTTCACCACCAAAGGTGTG
TTGGCTGGCAACAATCGGCAGGGTCAAGGGGAAGAAAGGGAGTGCCATTTACTTGGCTGGGGGTC
AGAGCCATCTGGCTTACAGGAATCTCGCAGCACAGTCAAGTTGCAATTTGACATGATGAGGGCCT
GTAACTTGATTGCCACCGTCGCCCTGACTGCTGGTCAACTCATCTTCCTGATGGGACTCATCGAG
CTGCCAATCGTTTCTCAGGATTCCGAGTGGTGGGAAGAAGCCATAGCTGCTGTATTCCAGCTGGC
TAGTTTTGTACTTGTCATCGGACTGGTGACCTTTTATCGAATTGGACCTTACACCCACTTGTCCT
GGTCCTGCTATCTGGACATTGTTGCCTGCCTGCTGGCTACCTTGGCAGCTGCTATCCTCATCTGG
AACATTCTCCATCGCCGAGAAGACTGCATGGCTCCCCGTGTCATTGTCATCA – (seq
incomplete; ca 62 nt upstream of stop codon)
```

B

Clp24 second MO		Fraction of embryos displaying the TD defect class # (%)			
		Control	Second MO		First MO
		SC 4ng	Clp24 2ng + 2ng p53 MO	Clp24 4ng + 4ng p53 MO	Clp24 first MO 4ng
class:	TD absent	0	5 (21%)	14 (52%)	3 (12.5%)
	10<TD<30%	0	4 (17%)	2 (7%)	1 (4%)
	30<TD<90%	0	8 (33%)	7 (26%)	17 (71%)
	TD normal	10 (100%)	7 (29%)	4 (15%)	3 (12.5%)
	Total N	*10 (100%)*	*24 (100%)*	*27 (100%)*	*24 (100%)*
Average TD length (% of 10-somite screening segment; mean ± SEM		100 ± 0	5 ± 0.81	3.3 ± 0.76	5.8 ± 0.62

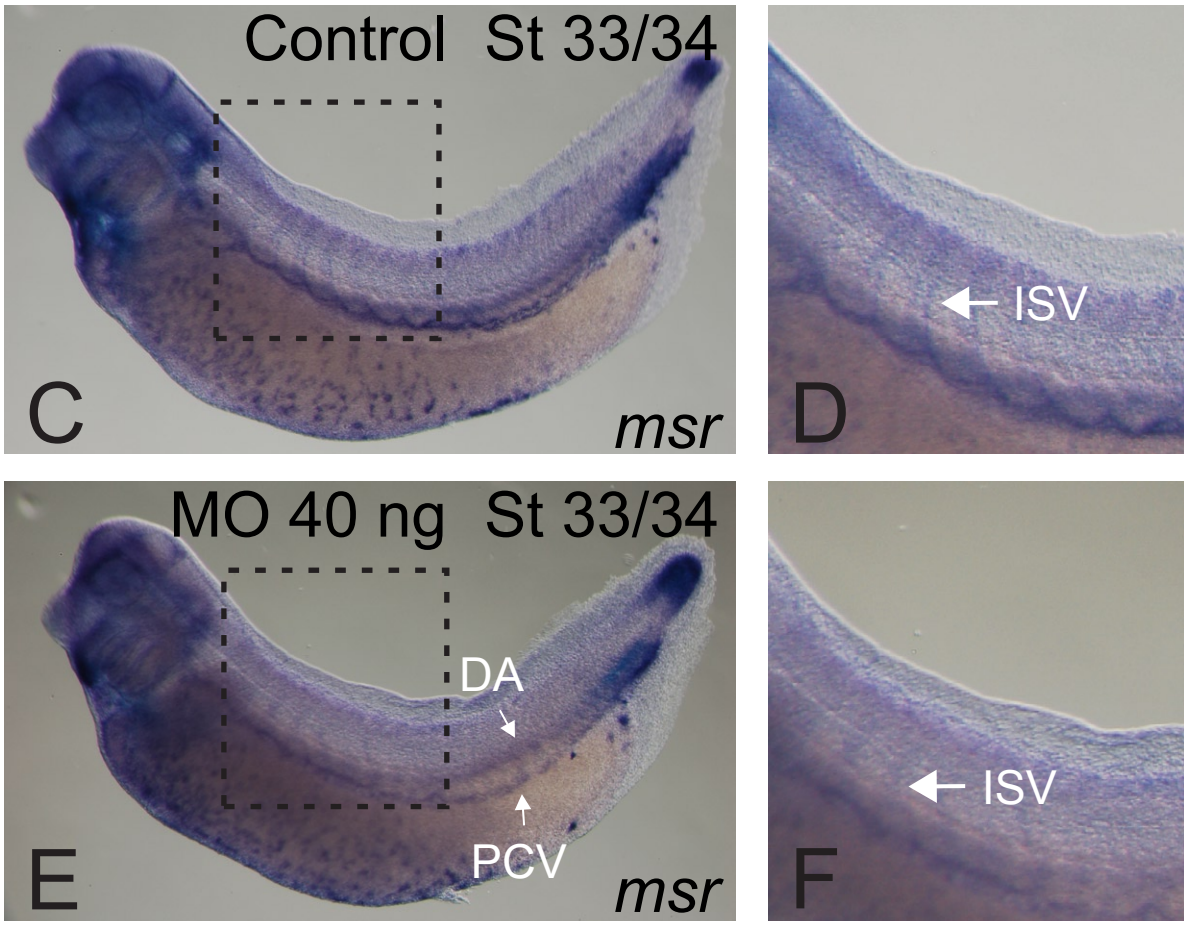
Control St 33/34
C
msr
ISV
D
MO 40 ng St 33/34
DA
PCV
E
msr
ISV
F

Saharinen_Fig S5.

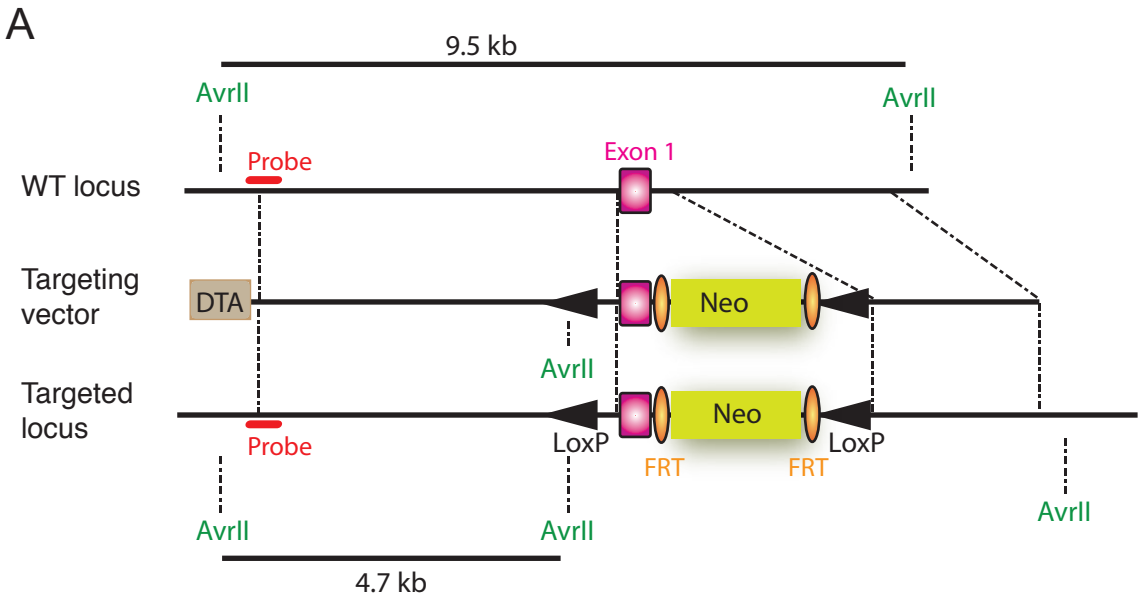

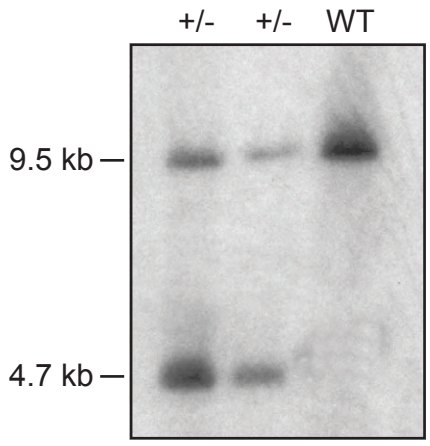

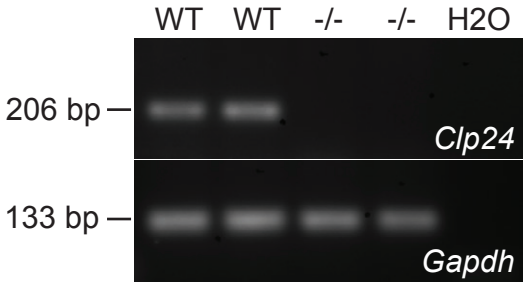

Saharinen_Fig S6.

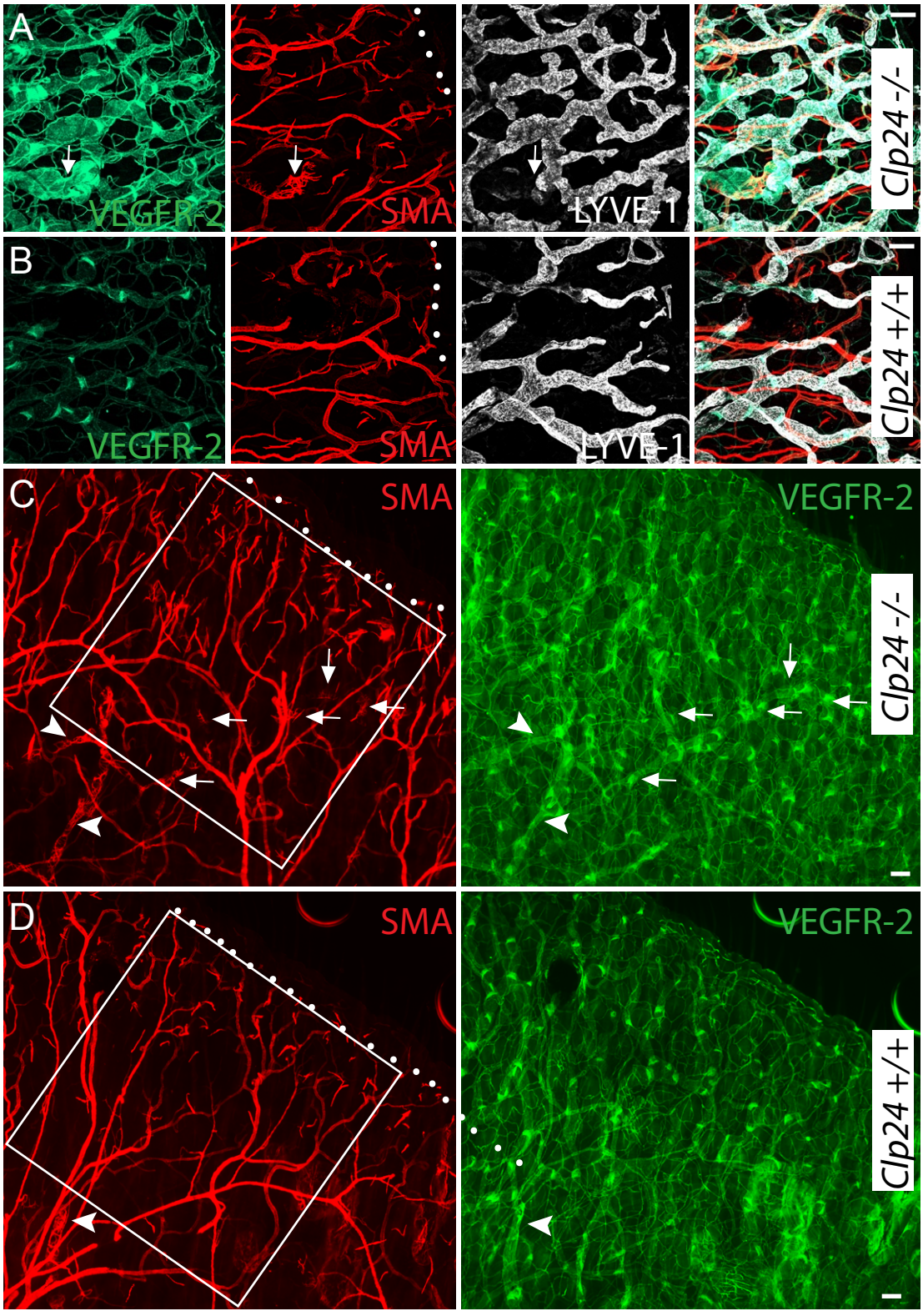

Saharinen_Fig S7.

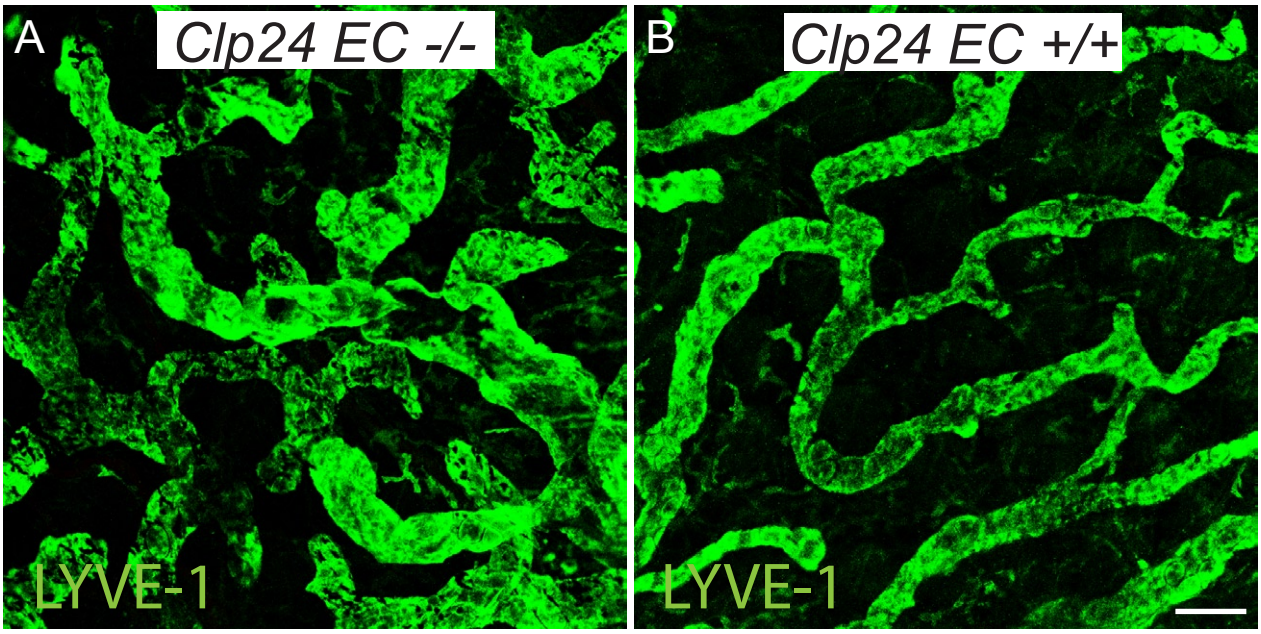

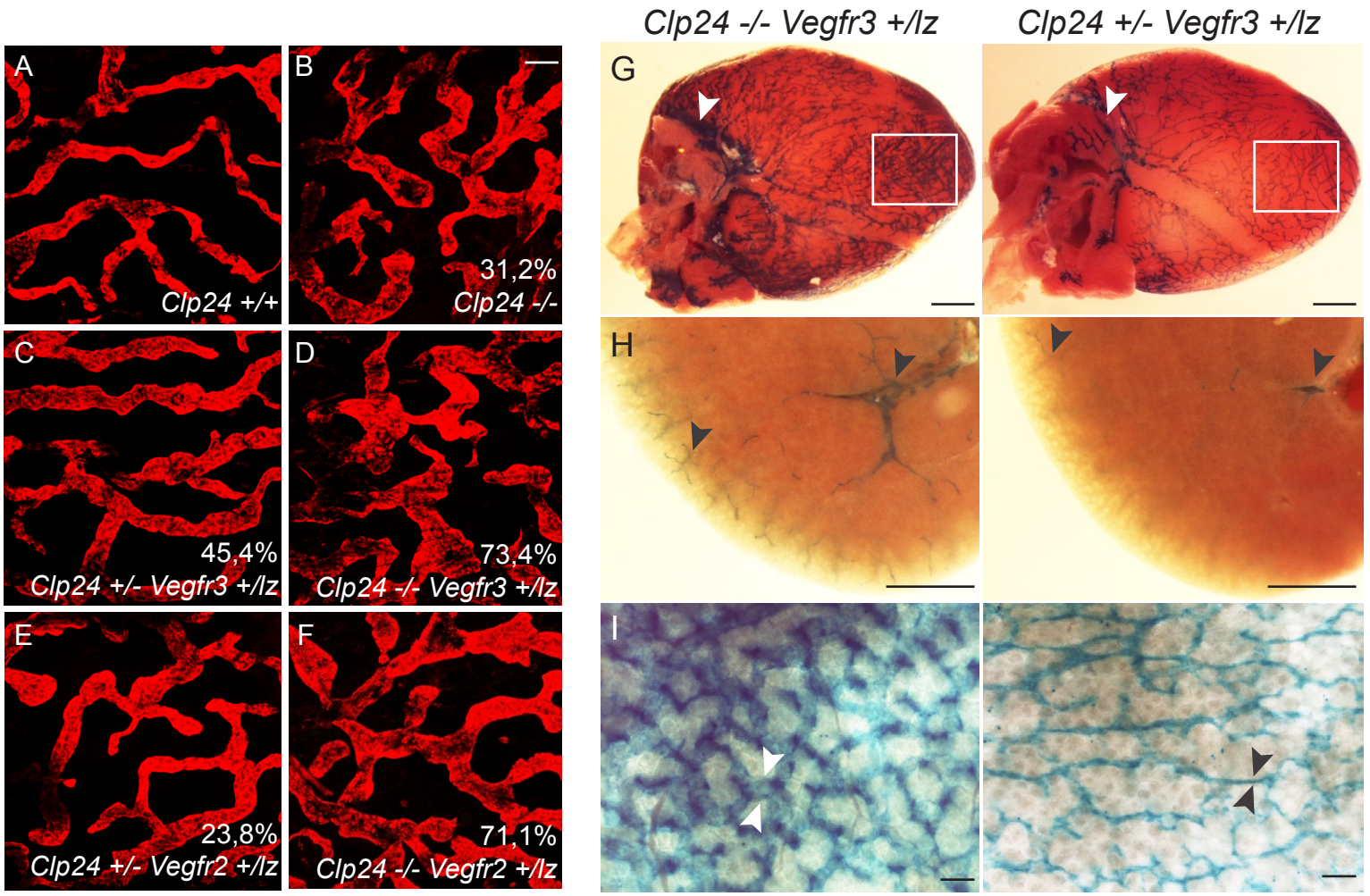
A
Clp24 +/+
B
31,2%
Clp24 -/-
C
45,4%
Clp24 +/- Vegfr3 +/lz
D
73,4%
Clp24 -/- Vegfr3 +/lz
E
23,8%
Clp24 +/- Vegfr2 +/lz
F
71,1%
Clp24 -/- Vegfr2 +/lz
Clp24 -/- Vegfr3 +/lz
Clp24 +/- Vegfr3 +/lz
G
H
I

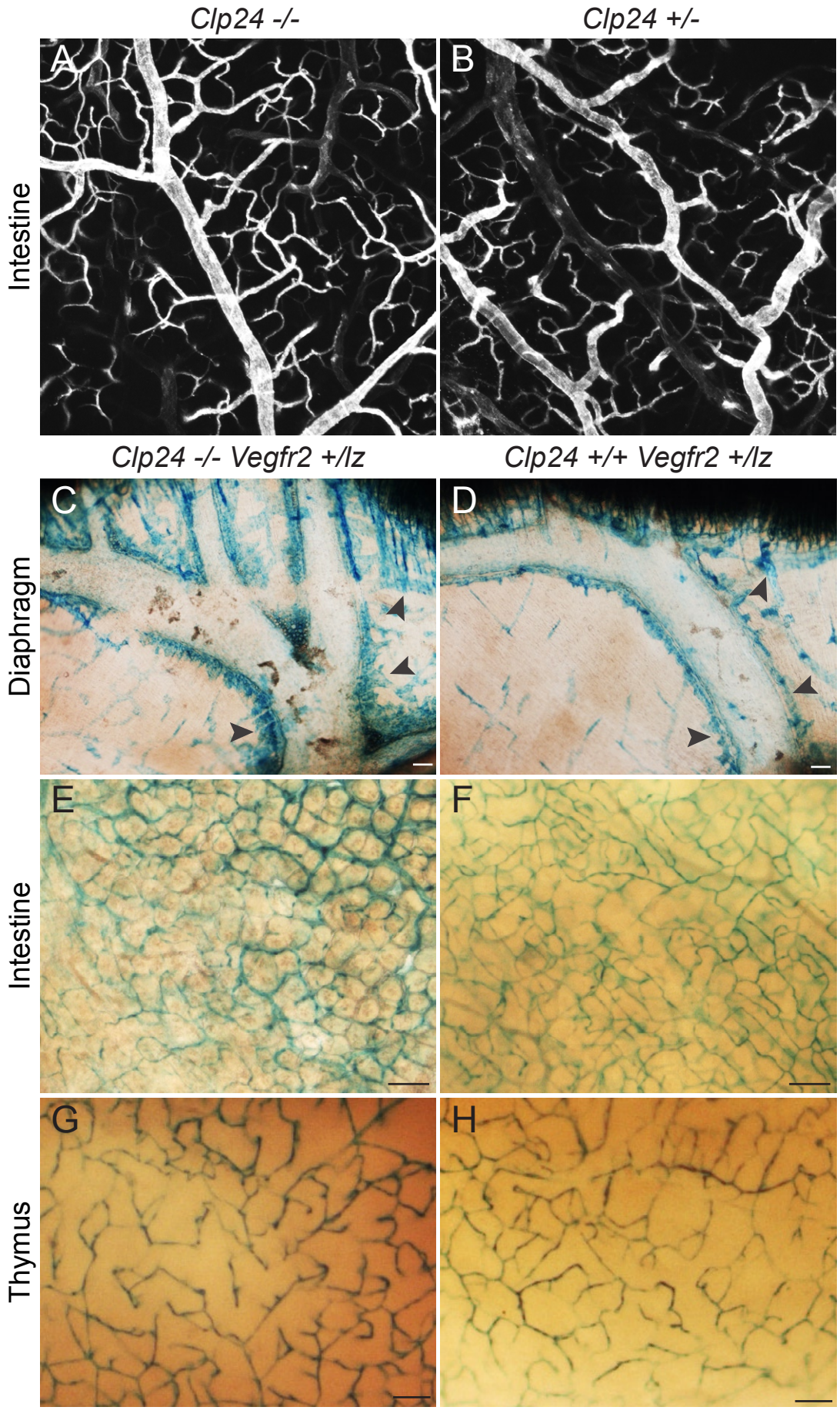
Clp24 -/-
Clp24 +/-
A
B
Intestine
Clp24 -/- Vegfr2 +/lz
Clp24 +/+ Vegfr2 +/lz
C
D
Diaphragm
E
F
Intestine
G
H
Thymus

A

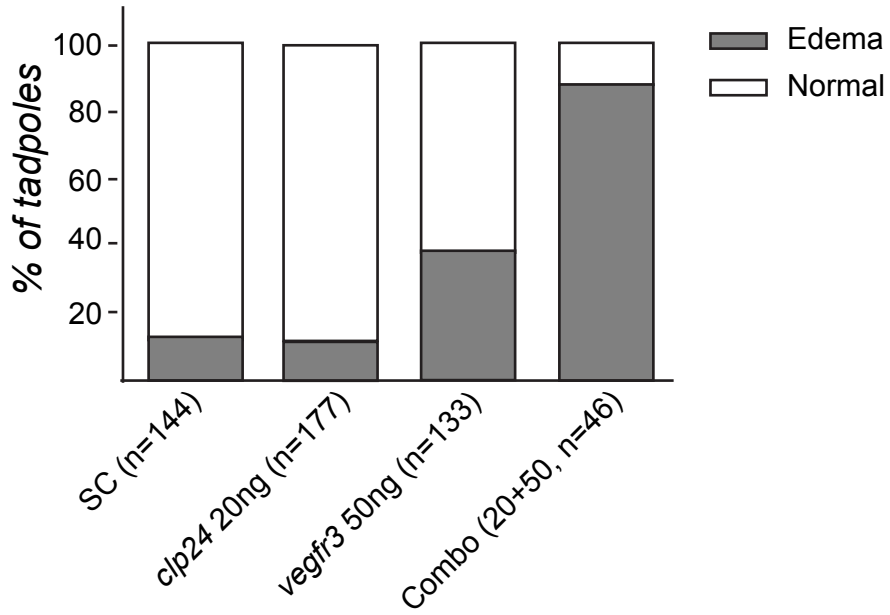
% of tadpoles
100
80
60
40
20
Edema
Normal
SC (n=144)
clp24 20ng (n=177)
vegfr3 50ng (n=133)
Combo (20+50, n=46)

B

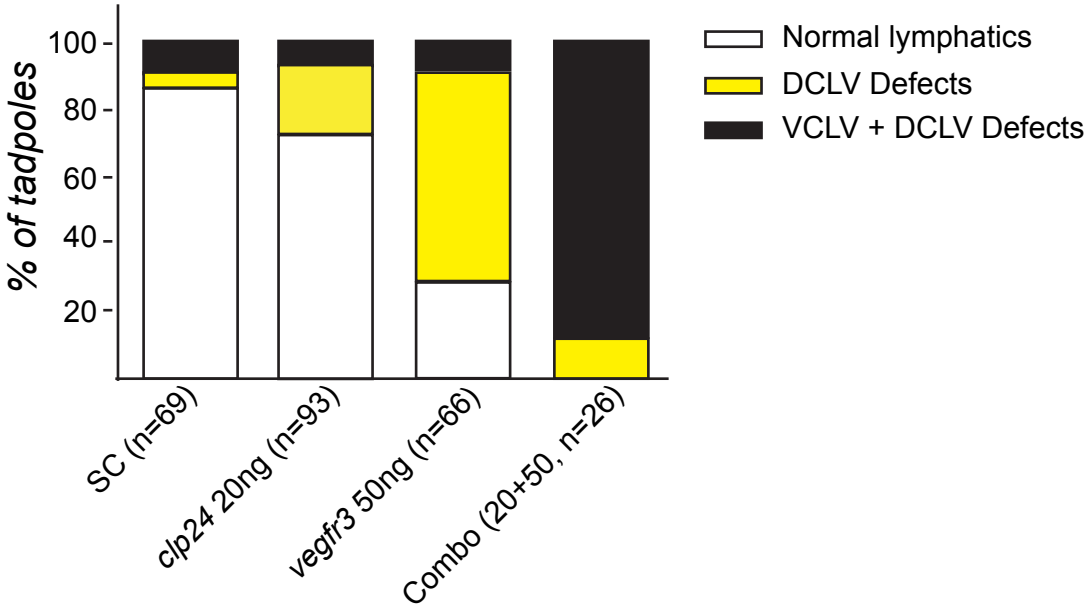
% of tadpoles
100
80
60
40
20
Normal lymphatics
DCLV Defects
VCLV + DCLV Defects
SC (n=69)
clp24 20ng (n=93)
vegfr3 50ng (n=66)
Combo (20+50, n=26)

Saharinen_Fig S11.